

Read-through compound 13 restores dystrophin expression and improves muscle function in the *mdx* mouse model for Duchenne muscular dystrophy

Refik Kayali¹, Jin-Mo Ku², Gregory Khitrov³, Michael E. Jung², Olga Prikhodko¹ and Carmen Bertoni^{1,*}

¹Department of Neurology, David Geffen School of Medicine, ²Department of Chemistry and Biochemistry and ³UCLA Molecular Instrumentation Center, Mass spectrometry Laboratory, University of California, Los Angeles, CA, USA

Received December 14, 2011; Revised and Accepted June 5, 2012

Molecules that induce ribosomal read-through of nonsense mutations in mRNA and allow production of a full-length functional protein hold great therapeutic potential for the treatment of many genetic disorders. Two such read-through compounds, RTC13 and RTC14, were recently identified by a luciferase-independent high-throughput screening assay and were shown to have potential therapeutic functions in the treatment of nonsense mutations in the ATM and the dystrophin genes. We have now tested the ability of RTC13 and RTC14 to restore dystrophin expression into skeletal muscles of the *mdx* mouse model for Duchenne muscular dystrophy (DMD). Direct intramuscular injection of compound RTC14 did not result in significant read-through activity *in vivo* and demonstrated the levels of dystrophin protein similar to those detected using gentamicin. In contrast, significant higher amounts of dystrophin were detected after intramuscular injection of RTC13. When administered systemically, RTC13 was shown to partially restore dystrophin protein in different muscle groups, including diaphragm and heart, and improved muscle function. An increase in muscle strength was detected in all treated animals and was accompanied by a significant decrease in creatine kinase levels. These studies establish the therapeutic potential of RTC13 *in vivo* and advance this newly identified compound into preclinical application for DMD.

INTRODUCTION

Duchenne muscular dystrophy (DMD) is a fatal X-linked recessive disorder that affects 1 out of 3500 liveborn males worldwide. Muscle weakening and wasting begins in early childhood, and progresses to wheelchair confinement by age 10. Death usually occurs between ages 20 and 30 by respiratory or cardiac failure as a consequence of the deterioration of the diaphragm and heart. The disease is caused by mutations in the dystrophin gene (1), 13% of which are nonsense mutations that generate a premature stop codon and that result in a truncated, nonfunctional, protein (2,3). Dystrophin is a critical component of the dystrophin-glycoprotein complex (DGC) in muscle that links the actin cytoskeleton to the extracellular

matrix of myofibers. The lack of a functional dystrophin protein causes loss of proper localization of many of the DGC components at the sarcolemma of muscle fibers leading to membrane instability and myofiber degeneration.

The *mdx* mouse is a widely used animal model of DMD. In this naturally occurring strain, a G-to-T transversion in exon 23 of the dystrophin gene converts a GAA codon into a UAA thus resulting in premature termination of protein synthesis and the absence of dystrophin expression in skeletal muscle (4). The *mdx* mouse displays similar muscle pathology to DMD patients, including susceptibility to muscle damage and degeneration. Studies involving *mdx* mice demonstrated that the restoration of as little as 20% of wild-type dystrophin protein abrogates the mouse pathology and infers that this

*To whom correspondence should be addressed at: Department of Neurology, University of California, Los Angeles, 710 Westwood Plaza, Los Angeles, CA 90095, USA. Email: cbertoni@ucla.edu

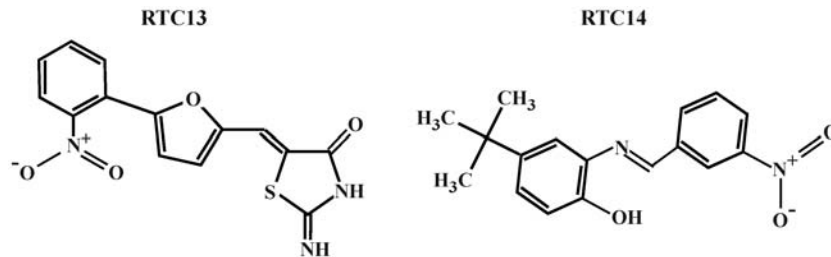


Figure 1. Molecular structures of RTCs. RTC13: (Z)-2-imino-5-((5-(2-nitrophenyl)furan-2-yl)methylene)thiazolidin-4-one and RTC14: 4-*tert*-butyl-2-[(3-nitrobenzylidene)amino]phenol.

level of protein expression may have significant beneficial effects on alleviating the symptoms of DMD patients (5).

Prior studies have demonstrated that aminoglycoside compounds such as gentamicin (6–11) can read-through premature stop codons and result in synthesis of the full-length protein. Among the three codons, UAA, UAG and UGA, which act as signals to terminate translation, the UAA codon is the most efficient and has little read-through activity. The UAG and UGA have lower fidelity and are therefore more amenable to read-through (12,13). Gentamicin interferes with normal ribosomal translation and proofreading activity, and substitutes a different amino acid for the premature termination codon (PTC), thus allowing the full-length protein product to be generated (14). Gentamicin underwent clinical trials in patients with DMD (10,15), and cystic fibrosis (16), and was shown to induce the expression of functional, previously missing, proteins in both diseases. However, the use of gentamicin is limited by the side effects associated with its long-term administration, including ototoxicity and nephrotoxicity, hampering its clinical applicability for the treatment of genetic disorders due to nonsense mutations. Nonetheless, these studies have served as proof-of-concept that such molecules can interfere with the nonsense-mediated decay (NMD) surveillance pathway on mRNAs containing premature stop codons and have paved the way for the discovery and development of new strategies aimed at discovering new drugs that could be used to treat disorders due to early termination of translation.

Two luciferase-based high-throughput screens (HTS) of nearly 800 000 low molecular weight compounds were used to identify a non-aminoglycoside compound, PTC124, capable of promoting ribosomal read-through of PTCs (17). The read-through compound (RTC) has been shown to be specific for PTCs and does not interfere with normal stop codons. Moreover, PTC124 was shown to induce more efficient read-through activity than previously used aminoglycosides (17). However, recent findings have demonstrated that the specificity of the HTS utilized for the identification of the RTC may have been compromised by the ligand-induced stabilization of the reporter protein used for the screen (18). Although other interpretations have been offered (19), strong evidences have been presented in support of the post-translational activity of PTC124 (20,21). Despite the off-target effects, PTC124 has been shown to suppress nonsense mutations in different disease models and has reached clinical testing in patients (17,22). However, the indeterminate efficacy of Ataluren (PTC124) in clinical trials for Duchenne boys supports the need of identifying new drugs that could be used to suppress nonsense mutations in the clinical scenario.

Recently, a sensitive and quantitative HTS method was developed by Du *et al.* (23) and used to screen low-molecular mass non-aminoglycoside compound libraries to identify potential drugs with PTC read-through activity. The screening protocol involved the use of a protein transcription/translation (PTT)–enzyme-linked immunosorbent assay (ELISA), using ataxia-telangiectasia (A-T) as a genetic disease model. This PTT–ELISA was driven by plasmid templates containing prototypic *ATM* mutations, patterned after specific disease-causing A-T (23). The screen of nearly 34 000 compounds led to the identification of RTC13 and RTC14 (Fig. 1). Both compounds have been shown to have biological activity in different lymphoblastoid cell lines derived from A-T patients containing each of the three types of nonsense mutations (TGA > TAA > TAG). Furthermore, RTC13 and RTC14 restored full-length dystrophin in *mdx* cells in culture (23). Altogether, these data demonstrated that the compounds had read-through activity on different types of proteins, in more than one species and cell lineage, and that their activity is independent of the location of the premature stop codon within the transcript. Furthermore, neither RTC13 nor RTC14 was shown to read-through normal termination codons thus confirming their specificity for PTCs (23).

In an attempt to further evaluate the potential of these compounds for the treatment of DMD, we tested their ability to restore dystrophin expression in skeletal muscles in *mdx* mice. Intramuscular injections of RTC13 promoted read-through of the *mdx* UAA stop codon more efficiently than gentamicin, PTC124 or RTC14, making it our lead drug candidate. Systemic administration of RTC13 restored dystrophin protein in all major muscle groups, including the diaphragm and heart. Dystrophin was significantly higher than that achieved by PTC124 and resulted in a significant increase in muscle strength over mice that did not receive the RTCs. The improvement in muscle function was paralleled by a decrease in creatine kinase (CK) levels, a marker of muscle degeneration. These data advance the development of RTC13 as an effective drug candidate for DMD. They also offer hope for the treatment of numerous other genetic disorders due to nonsense mutations and premature termination of protein synthesis.

RESULTS

Dystrophin protein expression in compound-treated *mdx* muscle cells

We have previously demonstrated that RTC13 and RTC14 were more efficient than gentamicin in restoring dystrophin

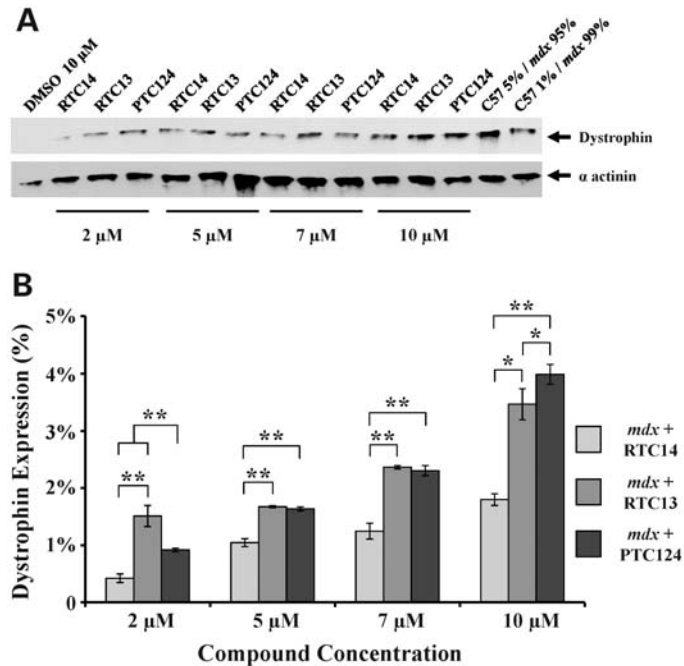


Figure 2. Dystrophin expression in *mdx* myotubes after exposure to RTCs. (A) Myoblasts were induced to differentiate for 16 h and then exposed to the compounds for an additional 80 h prior to protein analysis. Dystrophin was detected by western blot analysis in all cells treated with RTC13, RTC14 and PTC124 but not in cells exposed to DMSO or in untreated *mdx* myotubes. As positive control, 12.5 or 2.5 μg of protein isolated from wild-type myotubes maintained in differentiation media for the same period of time (corresponding to 5 or 1% of total protein) were mixed with proteins isolated from untreated *mdx* myotubes to a final concentration of 250 μg and then loaded. Equal loading was confirmed by western blot using α -actinin as internal control. (B) Quantitative analysis of protein levels was obtained from multiple independent experiments and showed a dose response increase in dystrophin expression in all compounds tested (* $P \leq 0.05$, ** $P \leq 0.004$).

expression in *mdx* myotubes (23). To further evaluate the clinical potential of these RTCs for DMD and to determine the optimal dose ranges at which the compounds would achieve maximal efficacy, we studied read-through activity of RTC13 and RTC14 on the dystrophin *mdx* mutation in cells in culture and compared those with PTC124. *Mdx* myoblasts were induced to differentiate for 16 h and compounds were added at a final concentration of 2, 5, 7, 10 and 20 μM for up to 3 days (4 days in differentiation media), as described in greater detail in the Materials and Methods. Western blot analysis revealed expression of full-length dystrophin in all cells treated with the RTCs but not in cells treated with vehicle. RTC13 was shown to better promote read-through activity than RTC14, consistent with the results previously published (23). Dystrophin was clearly detected in myotubes exposed to RTC13 and PTC124 at concentrations as low as 2 μM and increased in a dose-dependent manner (Fig. 2A). The levels of dystrophin protein restored were comparable among the three compounds, although RTC13 and PTC124 were able to better promote read-through of the *mdx* mutation than RTC14. Maximal read-through activity was achieved at a dose of 10 μM (Fig. 2B and Supplementary Material, Fig. S1).

Immunostaining analysis confirmed expression of dystrophin in myotubes treated with the RTCs. No expression was detected in untreated cells maintained in culture under similar conditions (Supplementary Material, Fig. S2). The intensity of the staining was much lower than that detected in wild-type myotubes maintained in differentiation media for the same period of time (data not shown). Nonetheless,

dystrophin protein could be detected in virtually every myotube present in the culture, suggesting that the compounds were readily taken up by cells.

Dystrophin expression in muscle fibers after intramuscular delivery of compounds

To demonstrate the effect of compounds *in vivo*, tibialis anterior (TA) muscles of *mdx* mice were injected with RTC13 or RTC14. Dystrophin expression was assessed 2 weeks later as previously described (24–26). Gentamicin and PTC124 were included in these studies as additional internal controls. No dystrophin was detected in TA muscles injected with vehicle (Fig. 3). Dystrophin-positive fibers were detected in all TA muscles injected with RTC13 or PTC124. In those muscles, dystrophin could be detected along the entire length of the muscle being examined, although the intensity of the staining was lower than that detected in wild-type TA. Notably, muscles injected with PTC124 showed a patchier dystrophin staining restricted primarily into clusters of positive fibers scattered throughout the section. Muscle injected with RTC13 showed broad distribution of dystrophin-positive fibers per cross-sectional area. RTC14 had only limited activity *in vivo*. Weakly dystrophin-positive fibers were only detected in a small percentage of the fibers targeted by injection of RTC14 (Fig. 3A). Similarly, muscles that received gentamicin showed low, although detectable levels of dystrophin (Fig. 3A). Taken together, these data suggest

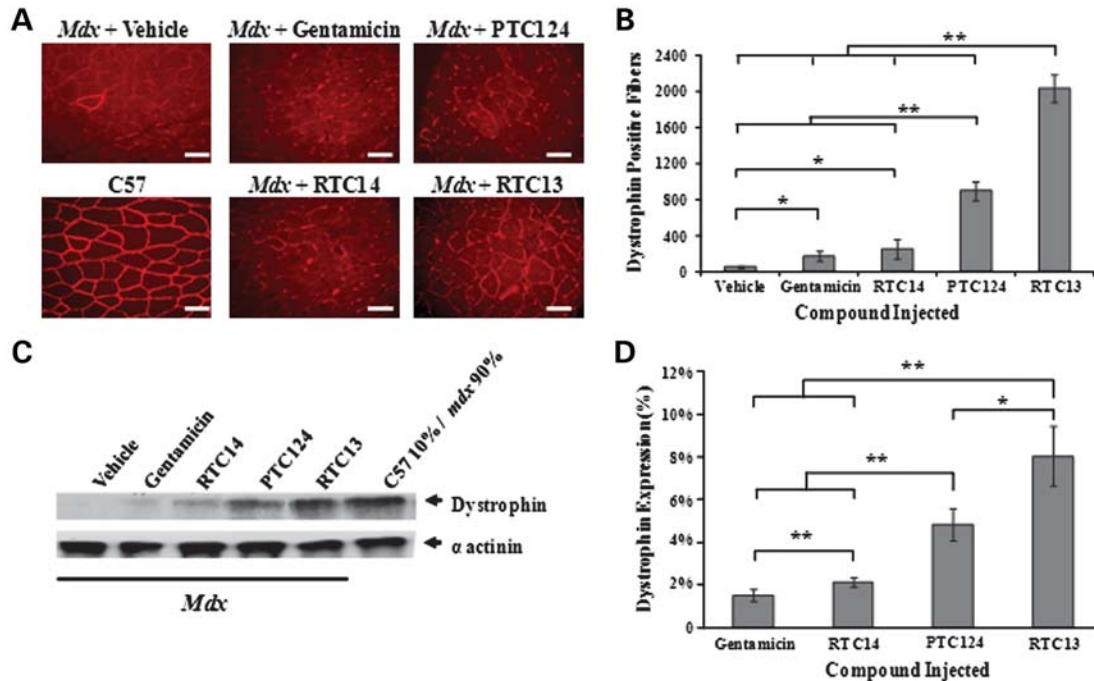


Figure 3. Single dose intramuscular injection of RTCs. (A) Dystrophin staining in TA muscles of *mdx* mice injected with RTC13, RTC14, gentamicin or PTC124 and analyzed 2 weeks after delivery of compounds and compared with muscles treated with DMSO alone. Dystrophin expression was evident in muscles that received RTC13 and, to a lesser extent, in muscles injected with PTC124 but not in sham-injected muscles. Weak expression was detected in TA muscles injected with gentamicin and RTC14. ($N = 4$ muscles per compound; scale bar: 50 μm). (B) The number of dystrophin-positive fibers was determined across the length of the muscle. TA injected with RTC13 showed a significantly higher number of positive fibers than muscles that received gentamicin, RTC14 or PTC124. Shown here is the average number of dystrophin-positive fibers per cross-sectional area containing the highest number of positives. ($N = 4$ muscles per compound; $*P < 0.04$; $**P < 0.002$). (C) Western blot analysis was used to detect full-length dystrophin expression in muscles injected with the compounds and analyzed for dystrophin 2 weeks later. Protein isolated from wild-type TA muscles was used as positive control to visualize dystrophin and was diluted with total protein isolated from *mdx*-untreated muscle (10% of total wild-type protein and 90% of total *mdx* protein for a final concentration of 250 μg). Here shown are the representative results of three independent experiments. (D) The level of dystrophin protein was significantly higher in muscles injected with RTC13 than those that received gentamicin, RTC14 and PTC124 ($*P \leq 0.03$, $**P \leq 0.002$).

that neither gentamicin nor RTC14 may be ideal drug therapeutics for the treatment of DMD patients.

Results were confirmed by western blot analysis of dystrophin expression. Limited or no protein was detected in muscles that received gentamicin or RTC14. Muscles injected with PTC124 and RTC13 showed a clear band of identical molecular weight when compared with that detected in samples isolated from wild-type TA muscles (Fig. 3C). Full-length dystrophin expression remained significantly higher in muscles injected with RTC13 when compared with those treated with PTC124 and showed levels of expression of up to 8% of that of wild-type muscles (Fig. 3D).

Full-length dystrophin expression restores the DGC

It is well documented that a defective protein within the DGC leads to the secondary loss of other members within the complex (27). To determine whether the dystrophin protein being restored was functionally active, we immunoassayed consecutive sections isolated from treated TA muscles using an antibody specific to β -dystroglycan (Supplementary Material, Fig. S3). No β -dystroglycan expression was detected in untreated or sham-injected *mdx* muscles and only sporadic weakly positive fibers were detected in muscles injected with gentamicin or RTC14. Muscles that received PTC124 showed

a much brighter β -dystroglycan staining than gentamicin- or RTC14-treated muscles. Immunostaining was confined only to those clusters of fibers shown to be dystrophin-positive. β -Dystroglycan was clearly expressed at the myofibers of muscles treated with RTC13 and was widely distributed throughout the cross-sectional area of muscle sections. Its distribution was similar to that observed after dystrophin immunostaining (Supplementary Material, Fig. S3). Altogether, these data demonstrated that only RTC13, but not RTC14, was capable to efficiently read-through the premature stop codon and to restore functionally active dystrophin protein in muscles of *mdx* mice, consistent with the results obtained by immunohistochemistry analysis of dystrophin expression.

Tolerability and toxicology studies of RTC13 in wild-type mice

Studies were used to determine the overall effects and toxicity of RTC13 after intraperitoneal administration and were conducted in wild-type (C57BL/10) mice at 10 to 12 weeks of age. For the acute toxicity studies, mice ($N = 20$) were divided into four groups that received RTC13 at escalating doses of 10 ($n = 5$), 30 ($n = 5$), 60 ($n = 5$) or 300 mg/kg ($n = 5$). Mice were sacrificed 5 days after injection. All animals were observed daily for signs of overt toxicity based

on behavioral changes, motility and changes in body weight. Results were compared with those obtained in untreated mice or mice that received vehicle alone. No clinical signs of toxicity were observed in animals following treatments. Furthermore, no significant differences in body weight were detected in any of the groups that received RTC13 compared with controls animals (data not shown). The serum level of albumin, alkaline phosphatase (ALP), creatinine, alanine aminotransferase (ALT), total bilirubin, lactate dehydrogenase, blood urea nitrogen (BUN), cholesterol, total protein and glucose were all within the normal range. Minimal histopathological changes were detected in the kidney of treated animals which showed glomerular mesangial proliferation and congestion restricted primarily to the group of mice that received the 300 mg/kg dose. No degenerative changes were detected in liver of treated animals when compared with mice that received vehicle alone.

The toxicity of RTC13 after repeated administration was assessed at a dose of 30 mg/kg, the minimal dose necessary to elicit significant read-through activity in dystrophin-deficient mice as demonstrated empirically through pilot studies. The injection regimen in mice, was chosen based on the Maximum Tolerated Dose (MTD) of vehicle as described in greater detail in the Materials and Methods. Wild-type mice received six injections of RTC13 intraperitoneally (one every 5 days) over a period of 4 weeks. The control group received the vehicle [dimethyl sulfoxide ((DMSO))] alone with the same regime. Mice were monitored daily for signs of toxicity as described above and were sacrificed 2 weeks after the last injection. Behavioral changes were not observed in any of the experimental groups. Similarly, no changes were detected in total body weight in treated animals when compared with controls. Serum biomarkers of liver and kidney damage were all within the normal range and no changes in the CK levels were detected in mice that received RTC13 compared with untreated or sham-injected mice. No changes were observed in liver and kidney weights at the time of necropsies, and Hematoxylin and Eosin (H&E) staining revealed the absence of histopathological changes (data not shown).

Systemic administration of RTC13 in *mdx* mice

The therapeutic potential of RTC13 for DMD after systemic administration was assessed in young (4 weeks of age) *mdx* mice that received the compound at a dose of 30 mg/kg. Compound was injected every 5 days over a period of 4 weeks (six injections in total). Muscles were isolated 3 weeks after the last injection. PTC124 was used as a control and was administered in age-matched *mdx* mice at the same dose regimen. Body weight was assessed daily and was used as an index of compound tolerability *in vivo* after prolonged exposure. No significant differences were found in average body weight in RTC13-injected mice or in mice injected with vehicle throughout the duration of the experiment (data not shown).

Dystrophin-positive fibers were detected in muscles isolated from mice that received RTC13 and PTC124 (Fig. 4 and Supplementary Material, Fig. S4). The distribution of dystrophin-positive fibers varied widely among different muscle groups, suggesting differences in compound uptake into those

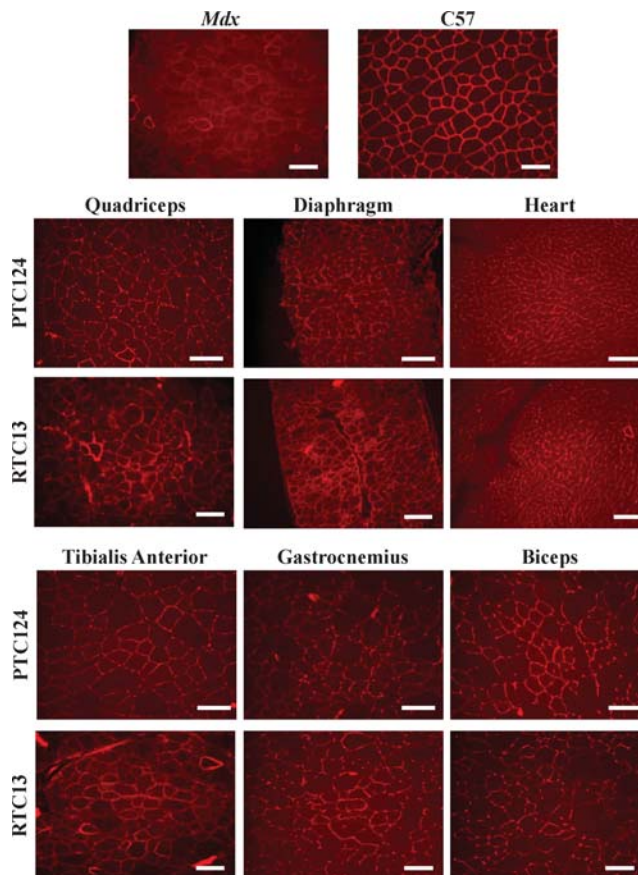


Figure 4. Dystrophin expression after systemic administration of RTC13. The efficacy of RTC13 and PTC124 to restore dystrophin expression after systemic administration was assessed in *mdx* mice at 4 weeks of age. Animals were injected intraperitoneally with compounds at a concentration of 30 mg/kg for 4 weeks with a wash out period of 5 days between each treatment. Mice were allowed to recover for 3 weeks and muscles were analyzed for dystrophin expression. Dystrophin was widely distributed throughout the muscle, although the level of dystrophin expression differed among muscle groups. The intensity of the staining was lower than that detected in muscles of wild-type mice. The immunostaining of a wild-type (C57) quadriceps muscle is shown for comparison. RTC13 showed broader distribution of dystrophin expression than PTC124 in all muscles analyzed ($N = 4$ mice per treatment group; scale bar: 100 μm).

muscles. Large clusters of positives were often localized within the same area of each muscle group, indicating that uptake of compounds into myofibers varied also within different regions of the same muscle. The number of dystrophin-positive fiber was significantly higher in muscles isolated from mice that received RTC13 when compared with mice injected with PTC124 (Fig. 5A). The differences in the number of dystrophin-positive between muscles of RTC13- and PTC124-treated mice were consistent in all sections analyzed and along the length of the muscle. Western blot analysis confirmed the expression of full-length dystrophin in all muscles analyzed and isolated from RTC13-treated mice (Fig. 5B and Supplementary Material, Fig. S5). The level of the dystrophin protein ranged between 0.5 and 5% depending on the muscles being analyzed and the RTC used. However, the level of dystrophin expression remained higher in muscles isolated from RTC13-injected mice than those

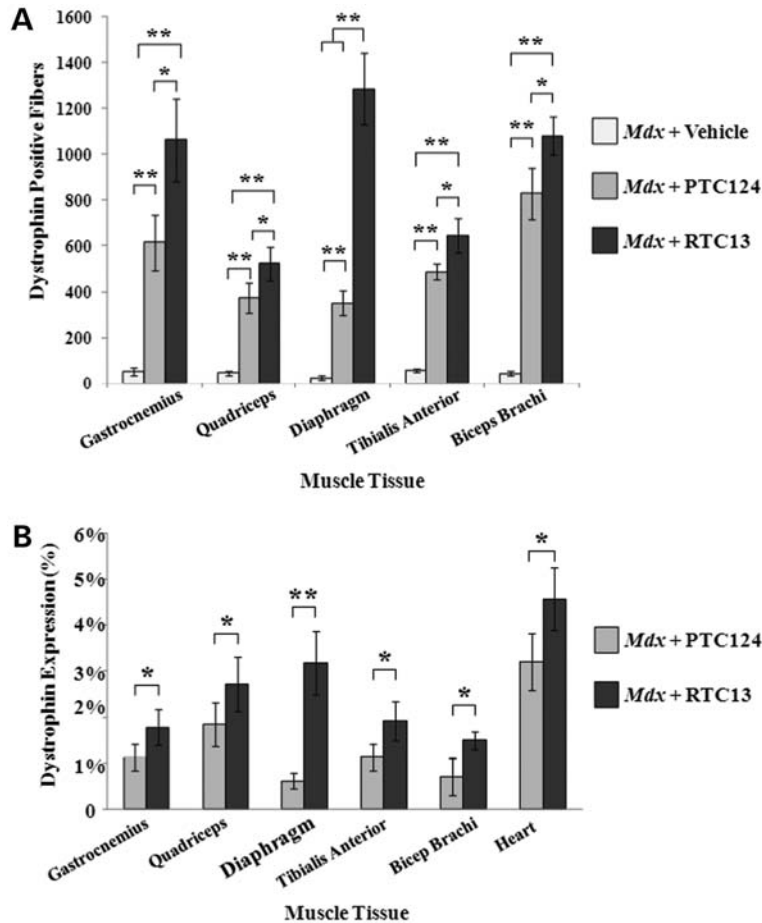


Figure 5. Quantitative analysis of dystrophin expression after systemic administration. (A) Average number of dystrophin-positive fibers per cross-sectional area containing the highest number of positives. Dystrophin-positive fibers were detected throughout the entire length of the muscle being examined. Muscles injected with RTC13 consistently showed a significantly higher number of dystrophin-positive fibers than muscles of mice that received PTC124 ($N = 4$ mice per treatment group; $*P \leq 0.05$, $**P \leq 0.004$). (B) Dystrophin expression was consistently higher in muscles of *mdx* mice that received RTC13 when compared with those treated with PTC124. Protein was prominent in quadriceps, diaphragm, gastrocnemius and heart muscles of RTC13-injected mice. No dystrophin expression was detected in muscle groups isolated from *mdx* mice that received vehicle alone. Results were consistent among triplicate experiments ($*P \leq 0.05$, $**P = 0.001$).

isolated from mice that received PTC124 (Fig. 5B and Supplementary Material, Fig. S5).

To further confirm that the amount of dystrophin achieved after treatment with RTC13 was functionally active, muscle sections were immunoassayed for β -dystroglycan expression (Supplementary Material, Fig. S6). Positive fibers were clearly detected in muscle fibers that received RTC13 intraperitoneally and that were positive for dystrophin. No β -dystroglycan expression was detected in mice that received vehicle only.

Evidence of partial recovery of muscle function after administration of RTC13

Despite the lack of a severe phenotype in the *mdx* mouse, subtle weakness can be quantified by a number of measures, including forearm grip strength and hanging tests (28,29). To assess whether compound injection could alter the course of muscular dystrophy in the *mdx* mouse, we examined young mice for the evidence of improvement in muscle

strength (Fig. 6A and B). Mice were subjected to the same intraperitoneal dose regimen described above and functional testing was performed 3 weeks after the last compound administration. For the forelimb grip strength test, five trials were performed with a minimum of 30 s rest in between. Values were averaged to calculate absolute strength, which was divided by the body weight in grams (Fig. 6A). The average peak tension normalized to body weight was ~ 2 -fold higher than that of vehicle-treated mice, although it was still statistically significantly lower than that obtained in wild-type mice ($P < 0.05$). Furthermore, a significant improvement in forelimb strength was detected in all mice that received RTC13 when compared with PTC124-treated animals (Fig. 6A).

Overall body coordination and strength were tested by a four-limb hanging wire test (30–32). A significant improvement was detected in mice that received the RTCs when compared with sham-injected mice (Fig. 6B). No differences were detected in the results obtained in mice treated with RTC13 compared with mice that received PTC124.

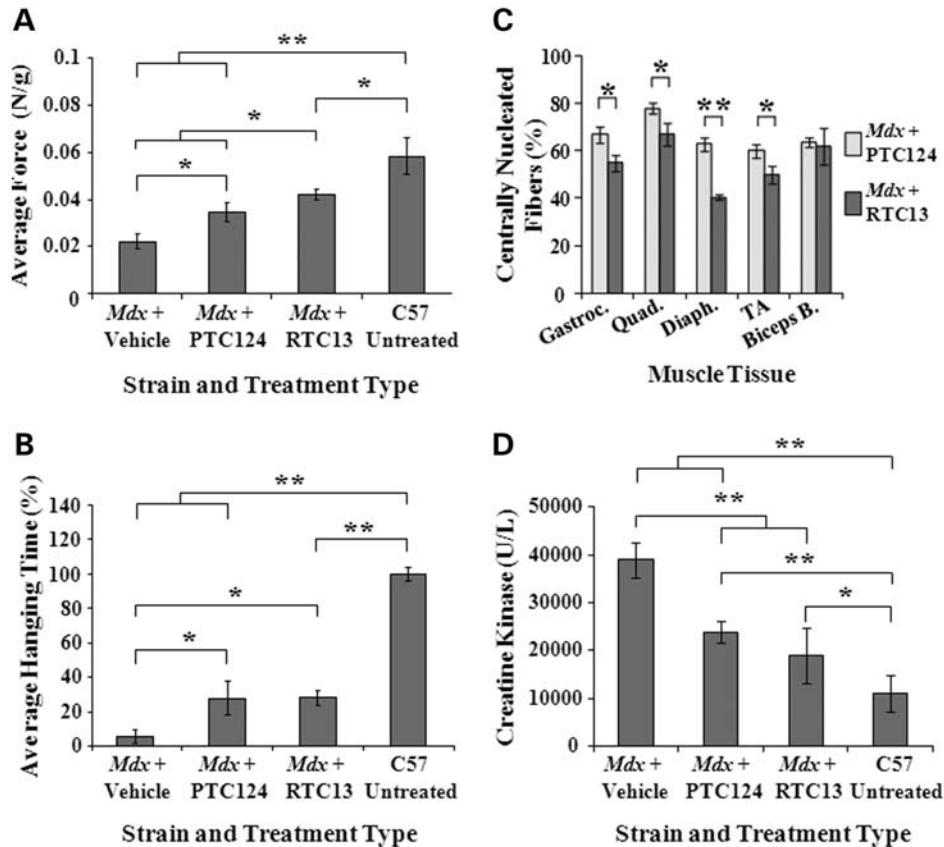


Figure 6. Functional improvement in *mdx* mice after treatment. (A) The forelimb grip test was used to assess the effects of systemic administration of RTCs on muscle strength. A significant force recovery was detected in *mdx* mice treated with RTC13 compared with sham-injected control mice and mice that received PTC124. Muscle strength remained significantly lower than that detected in wild-type mice. Similar results were obtained in duplicate experiments ($N = 5$ mice per treatment group; $*P < 0.05$; $**P < 0.005$). (B) Mice that received PTC124 or RTC13 showed a significant improvement in the ability to hang on a wire compared with sham-injected mice. Results were confirmed in duplicate experiments ($N = 5$ mice per treatment group; $*P < 0.05$; $**P = 0.002$). (C) The percentage of dystrophin-positive fibers containing central nuclei were quantified in gastrocnemius, quadriceps, diaphragm, TA and biceps brachii muscles isolated from mice that received RTC13 or PTC124 and was used as a measure of myofiber stability. Muscles of RTC13-injected mice showed a significant lower number of positive fibers containing central nuclei compared with muscles of *mdx* mice that received PTC124 ($N = 4$ mice per treatment group; $*P < 0.02$; $**P \leq 0.002$). (D) A significant difference in the levels of serum CK was detected only in *mdx* mice that received RTCs. No significant differences were detected in the CK levels of mice that received RTC13 compared with PTC124-injected mice ($N = 4$ mice per treatment group; $*P < 0.05$; $**P \leq 0.001$).

Improvements in muscle morphology were assessed in cross-sections of muscles isolated from *mdx* mice that received PTC124 or RTC13 and immunoassayed for dystrophin. Three weeks after the last injection, the majority of the dystrophin-positive fibers showed to contain central nuclei indicative of an ongoing process of regeneration characteristic of *mdx* mice. Nonetheless, the percentage of centrally nucleated myofibers positive for dystrophin was significantly lower in gastrocnemius, quadriceps, diaphragm and TA muscles isolated from *mdx* treated with RTC13 compared with that of muscles of PTC124-treated mice (Fig. 6C).

No significant differences were detected in the myofiber area of muscles that received RTC13 or PTC124. Frequency histograms showed subtle differences in the size distribution of myofiber that expressed dystrophin. A modest, although detectable shift toward less hypertrophic fibers was evident in dystrophin-positive fibers of muscles of RTC13-injected mice when compared with those detected in muscles isolated from mice that received PTC124 (Supplementary Material, Fig. S7).

To further validate the therapeutic effects of systemic delivery of RTC13, serum samples isolated from *mdx* mice injected systemically with RTC13 or PTC124 were analyzed for CK levels (Fig. 6D). CK levels are a widely accepted index of ongoing muscle damage and they have been used extensively to evaluate the efficacy of various treatments, including pre-clinical drug testing in *mdx* mice. CK values are subjected to large variations depending on the method of blood collection used and the methods employed among different laboratories (33). Due to those variations, the overall effectiveness of the evaluation is limited to a comparison of measured levels rather than the actual values obtained (33,34). In C57BL/10 and *mdx* mice, the CK values averaged to ~ 10000 and 40000 U/l respectively, consistent with the results obtained by others (35). Although these values were higher than those generally observed in other studies, they were consistent among different samples analyzed and in multiple independent experiments. No differences were detected between *mdx* mice that received vehicle only compared with untreated *mdx* mice (data not shown). Mice that received

RTC13 or PTC124 showed a significant decrease in the CK enzyme compared with vehicle-treated mice (Fig. 6D).

Distributions of PTC124 and RTC13 following intraperitoneal injection

Mdx mice were administered a single intraperitoneal injection of RTC at a dose of 30 mg/kg (Supplementary Material, Figs S8 and S9). Distribution of RTCs was followed for up to 5 days after injections. RTC13 was not detected in plasma regardless of time point analyzed, suggesting that RTC13 is rapidly cleared from blood after intraperitoneal administration (data not shown). The concentrations of PTC124 in plasma were similar to those previously reported after intraperitoneal injection and using a similar dose (17).

The liver and kidney exhibited high retention of both RTCs (Supplementary Material, Fig. S8B and C). A peak in RTC concentrations was detected 30 min after injection (the earliest time point analyzed) and remained high for up to 4 h after administration. During this period, the levels of PTC124 detected in both organs were significantly higher than those identified in tissues of RTC13-treated animals. Compound concentrations decreased drastically at 24 h and 5 days after administration but were still detectable in livers. RTC13 was absent in the kidney 5 days after injection (Supplementary Material, Fig. S8C).

We next determined the biodistribution of RTC13 and PTC124 in cardiac and skeletal muscles. Compounds were isolated from the heart, diaphragm, TA, quadriceps, gastrocnemius and biceps brachii muscles of *mdx* mice after single intraperitoneal injection of RTCs (Supplementary Material, Fig. S9). RTC13 and PTC124 showed to be readily taken up into those tissues. Distribution and rate of clearance of the RTCs were similar among the different muscle group and showed to be highest within the first few hours following administration. At the earliest time point analyzed, the concentrations of PTC124 were consistently 10- to 100-fold higher than that detected in muscles of RTC13-treated mice.

Absence of histopathological changes in *mdx* mice after RTC13 systemic administration

To evaluate possible cytotoxicity of RTC13, blood was collected after treatment and serum enzymes were used as indicators of liver and kidney damage (Supplementary Material, Fig. S6A–E). The levels of direct bilirubin (DBIL), BUN, creatinine and ALT were significantly higher in *mdx* when compared with C57BL/10 mice consistent with the results obtained by others (36). Mice that received RTC13 all showed a significant decrease in DBIL, BUN and creatinine when compared with untreated *mdx* mice or mice that received vehicle alone (Supplementary Material, Fig. S11). Statistically significant differences in the ALP levels were also detected in untreated *mdx* mice or *mdx* mice that received vehicle or RTC13 when compared with wild-type mice (data not shown). However, the levels remained within normal ranges. No statistically significant differences were detected in BUN, creatinine and ALP values of serum collected from RTC13-treated mice and compared with wild-type control mice.

Histological analysis using H&E staining of liver and kidney tissues isolated from *mdx* mice that received RTC13 systemically revealed the absence of morphological changes when compared with age-matched control mice (Supplementary Material, Figs S7 and S8). Altogether, these data demonstrated that the systemic administration of RTC13 had no toxic effects on liver and kidney functions in mice.

DISCUSSION

In this study, we have tested the ability of RTC13 and RTC14 to read-through the premature stop codon in the *mdx* mouse model for DMD and compared their efficacy in restoring full-length dystrophin expression to that of gentamicin or PTC124. Our results clearly indicate that of the two lead compounds identified by PTT–ELISA (23), only RTC13 warrant further drug development. Results obtained *in vitro* demonstrated a dose-dependent response in *mdx* myotubes treated with the compounds and ranged between 1 and 5% of that of wild-type dystrophin (Fig. 2). Amounts as low as 2 μ M were sufficient to restore dystrophin protein and suggest that even low doses of the compounds are effective in eliciting read-through activity of the UAA PTC in the mouse dystrophin mRNA.

Intramuscular injection of the RTCs also resulted in restoration of dystrophin expression in *mdx* muscles, although the levels of expression differ widely depending on the compound being injected (Fig. 3). Muscles that received gentamicin or RTC14 showed low, although detectable levels of dystrophin (Fig. 3A), suggesting that neither compound may be ideal drug therapeutics for the treatment of DMD patients. Dystrophin expression was higher in muscles that received PTC124, although the number of dystrophin-positive fibers (Fig. 3B) and the overall levels of protein restored within the entire muscle (Fig. 3C and D) remained lower than those detected in TA muscles injected with RTC13. The significant decrease in the CK levels detected after systemic delivery of RTC13 (Fig. 6D) further demonstrates that repeated administration of RTC13 can slow myofiber degeneration and therefore myofiber turnover. The beneficial effects achieved after the systemic administration of RTC13 were not limited to slowing the progression of the disease, but were also evidenced by an increase in muscle strength (Fig. 6A and B) and an improvement in muscle morphology (Fig. 6C and Supplementary Material, Fig. S7), indicating that low amounts of dystrophin expression are capable of improving the overall muscle pathology characteristic of *mdx* (Fig. 6).

The significant increase in dystrophin expression detected in *mdx* mice that received RTC13 when compared with that observed in PTC124-treated mice (Figs 4 and 5) cannot be attributed to differences in distribution of the RTCs into muscles. In fact, the levels of uptake of PTC124 in those tissues were significantly higher ($P \leq 0.0001$) than that of RTC13 (Supplementary Material, Fig. S9).

Moreover, the results obtained in this study suggest that analysis of dystrophin expression *in vitro* alone is not a good predictor of the efficacy of a RTC. Parameters like penetrability of the compound into the myofibers, its ability to distribute along the length of the fiber and its stability once it

reaches its targets are all critical factors that contribute to the efficacy of a drug candidate.

The difference in the intensity of the dystrophin staining observed by immunohistochemistry within myofibers that received RTC13 to that of wild-type muscles (Figs 3 and 5) also suggests that ribosomal read-through activity was achieved only into a fraction of the mRNA transcripts processed for translation. These results are consistent to those obtained by western blot (Fig. 2) and immunohistochemistry analyses of cells exposed to the RTCs (Supplementary Material, Fig. S2) which demonstrated only partial restoration of dystrophin expression in *mdx* cultures. Factors like NMD and binding affinity of the compound for its target are likely to play an important role in determining the efficacy of the RTC to act as a suppressor of early termination of protein synthesis.

The underlying mechanisms of read-through activity of RTC13 are currently under investigation. It has been demonstrated that all of the known RTCs including gentamicin and PTC124 function by interfering with ribosomal translation and is possible that RTC13 acts through similar mechanisms (37). Furthermore, the observation that none of the drugs or compounds that have been identified to date, including RTC13, exerts read-through activity of normal termination of protein synthesis suggests the presence of a selectivity of the compounds for stop codons which are inserted within coding sequences (8,14,17,23,38). It is also important to note that while peptide elongation requires proofreading activity, termination of protein synthesis has high termination fidelity which is achieved without the help of a proofreading mechanism. Although those mechanisms are yet to be elucidated in detail, they appear to relay on the interplay of multiple proteins and factors such as the poly(A)-binding protein, eukaryotic release factors (eRFs), the ribosomal A site and even NMD (39–41). Thus, it is likely that a small molecule, although may be able to avoid premature termination of mRNA synthesis in a region upstream the normal stop codon and the poly adenylation site, may have limited or no effects on altering the termination of protein synthesis in the context of normal (full-length) transcription.

Before RTC13 can be delivered into the clinic, multiple parameters will have to be addressed. Pharmacokinetics and pharmacodynamics, drug metabolism, solubility and plasma stability of RTC13 will have to be refined so as to achieve maximal read-through activity while maintaining optimal safety profiles. Nonetheless, the results obtained after systemic delivery of RTC13 are encouraging and demonstrate that the compound is stable *in vivo* and distributes effectively to muscles after intraperitoneal administration. The fact that dystrophin could be detected in the diaphragm and heart also indicates that the compound has the ability of distributing into two of the most difficult muscles to target in DMD patients and may prevent the degeneration of cardiac and respiratory tissues which are ultimately responsible for the short lifespan of these patients.

Any drug that targets nonsense mutations is likely to have only temporary effects and will require repeated administration of the compound over prolonged periods of time, potentially the lifetime of the patient. Our current studies are focusing on determining the bioavailability of RTC13 after

oral administration and on optimizing the dose necessary to achieve sustained effects. Factors like pH stability into the stomach and ability of the compound to be efficiently absorbed from the intestinal walls and into the blood stream will have a major impact in the designing of an orally viable formulation of the drug. The new formulation would avoid the need of administering the compound intraperitoneally and would also allow better control of compound distribution into muscles. Issues of toxicity will have to be carefully addressed in anticipation of prolonged drug administration in human patients. Nonetheless, our results clearly demonstrate that RTC13 is well tolerated in mice and does not elicit toxicity even after repeated administrations.

Some consideration should also be given to the maximal efficacy that can be achieved by the treatment which correlates strongly with the stability of the protein being restored, i.e. dystrophin. Several lines of evidence have demonstrated that in the *mdx* mouse, the half-life of the dystrophin protein can vary widely (between 8 and 26 weeks) depending on the amount of dystrophin being restored, the distribution of the protein within the cross-sectional area of the muscle and even the longitudinal distribution of the dystrophin protein along the length of the fiber (24,42–45). Periodic administration of the RTC should result in a buildup of dystrophin protein within the first few weeks of treatment which should eventually plateau when the amount of dystrophin being restored equals the amount of protein being degraded as a result of normal dystrophin turnover or as the result of the turnover of the myofiber. It is difficult to predict the exact levels of the dystrophin protein that can ultimately be achieved by prolonged administration of RTC13 or whether the levels of dystrophin expression being restored will be sufficient to halt or at least ameliorate the progression of the disease. However, the results obtained in the current studies after systemic administration of compounds in mice suggest that even low doses of RTC13 administered for a limited number of treatments can have beneficial effects.

To date, there is no treatment for DMD and most of the approaches that are currently under development are designed to ameliorate the disease by improving muscle strength or by restoring shorter although still functional dystrophin protein. Clearly, an approach capable of restoring full-length dystrophin expression remains the ideal option to identify an effective therapy. Thus, the use of RTC13 to suppress early termination of protein synthesis holds promise and could ultimately result in the development of an effective treatment for DMD. Many other genetic diseases resulting from nonsense mutations should also benefit from RTC drugs. Among those, cystic fibrosis, β -thalassemia, Hurler syndrome and other types of genetic diseases in which partial restoration of protein expression have proven therapeutic relevance, are likely to become ideal target for RTC-based therapies.

MATERIALS AND METHODS

Mice

All experiments were performed on male *mdx* mice (C57BL/10ScSn-*mdx*) or male control C57 (C57BL/10SnJ) mice. Animals were obtained from the Jackson Laboratory and

were handled in accordance with the guidelines of the Administrative Panel on Laboratory Animal Care of the University of California, Los Angeles. For each strain to be used, animals were randomized to individual treatment groups prior to commencing the study and were assigned a unique identifier (ear-tag number).

Compound synthesis

Gentamicin was obtained from Invitrogen (Carlsbad, CA, USA). RTC13 (*Z*)-2-imino-5-((5-(2-nitrophenyl)furan-2-yl)methylene)thiazolidin-4-one and RTC14 (4-*tert*-butyl-2-[(3-nitrobenzylidene)amino]phenol) were purchased from ChemBridge Corporation (San Diego, CA, USA) or chemically synthesized by the synthetic medicinal chemistry lab of M. E. Jung. Materials were obtained from commercial suppliers and were used without purification. All the moisture-sensitive reactions were conducted under argon atmosphere using oven-dried glassware and standard syringe/septa techniques. The reactions were monitored by TLC on silica gel using UV light and visualization with a *p*-anisaldehyde staining solution. ¹H NMR spectra and ¹³C NMR spectra were measured at 400 and 100 MHz, respectively, with the data are reported in ppm (δ) from the internal standard (TMS, 0.0 ppm), using the standard abbreviations. The purity of the compounds was assessed by several methods: high-field proton and carbon NMR (lack of significant impurities), R_f values on TLC (lack of obvious impurities). PTC124 was prepared using a method similar to the one described by Welch *et al.* (17), and its spectroscopic data were identical to those reported.

Intramuscular injections

TA muscles of *mdx* mice (4 weeks of age) were injected with 50 μ l of compounds resuspended at a concentration of 15 mM in DMSO. Other controls included non-injected muscles and muscles injected with equal volumes of DMSO vehicle. Mice were sacrificed 2 weeks after injection to assess dystrophin gene correction and expression. Four animals were used for each compound tested. Muscles to be used for immunohistochemistry analyses were dissected and embedded in Tissue-Tek O.C.T. compound (Sakura Finetek USA Inc., Torrance, CA, USA), snap frozen in liquid nitrogen-cooled isopentane and stored at -80°C prior to sectioning.

Intraperitoneal injections

The MTD of vehicle was assessed in mice ($N = 40$) that received intraperitoneal administration of DMSO at a dose of 6 mg/kg, the quantity necessary to dispense RTC13. Animals were injected at intervals of either, once daily, or once every 2, 3 or 5 days, respectively, for up to 1 month. DMSO was well tolerated only in mice that received vehicle once every 5 days. This injection regimen was then chosen for all subsequent studies.

Mdx mice (4 weeks of age) were injected intraperitoneally with RTC13 or PTC124 (resuspended in DMSO) and injections were performed at a concentration of 30 mg/kg once every 5 days for 4 weeks. Sham-treated animals were injected with an equivalent volume of DMSO. Mice were examined

daily and weights recorded. Three weeks after the last treatment, mice were sacrificed by cervical dislocation. Tissues were isolated as described above and maintained in -80°C until analysis.

Cell culture and compound treatment

Cells were derived from limb muscle of neonatal *mdx* and C57 mice as previously described (23,24,46). For growth, cells were plated on dishes coated with 5 μ g/ml laminin (Life Technologies, Inc.) and maintained in growth medium (GM) consisting of Ham's F10 nutrient mixture (Mediatech, Herndon, VA, USA) supplemented with 20% fetal bovine serum, penicillin and streptomycin. Cell differentiation was induced by maintaining the cells in the low serum medium (differentiation medium) consisting of DMEM supplemented with 2% horse serum, penicillin and streptomycin. Myoblasts were plated in six-well dishes (1.5×10^5 cells/well), allowed to seed for 5 h and then induced to differentiate for 16 h prior to compound treatment. Compounds were resuspended in DMSO at a concentration of 100 mM and were added to the media at the final concentration indicated in Figure 1 and Supplementary Material, Figure S1. Fresh differentiation media containing the compounds were replaced every 24 h. Cells were lysed 96 h after induction of differentiation (72 h after addition of the compounds).

Western blot analysis

Dystrophin immunoblot analysis in *mdx* myotubes was performed using 250 μ g of total protein isolated from cultures maintained in differentiation media for 3 days. Protein isolated from the wild-type (C57BL/10SnJ) was used as control. Cells were lysed in RIPA buffer (50 mM Tris-HCl, pH 7.4, 150 mM NaCl, 0.5% deoxycholate and 1% Nonidet P-40) containing aprotinin (20 μ g/ml), leupeptin (20 μ g/ml), phenylmethylsulfonyl fluoride (10 μ g/ml) and sodium orthovanadate (1 mM). Total protein in the extract was determined by the Bio-Rad protein assay (Bio-Rad, Hercules, CA, USA). Samples were separated by electrophoresis (10 mA for 15 h) using 5% SDS-polyacrylamide gels, and then transferred (250 mA for 7 h) onto nitrocellulose membranes. Membranes were blocked with 5% evaporated milk (Fisher Scientific, Pittsburg, PA, USA) in PBS for 1 h at room temperature and then probed overnight at 4°C with an antibody directed toward the rod domain (MANDYS -8; Sigma, St Louis, MO, USA; 1:400) of the dystrophin protein (24). Blots were washed with 0.05% Tween-20 in PBS and then incubated with a horseradish peroxidase-coupled anti-mouse secondary antibody (GE Healthcare Life Sciences Pharmacia Biotech, Piscataway, NJ, USA). Specific antibody binding was detected using an enhanced chemiluminescent system (Amersham).

Expression of the dystrophin protein *in vivo* was assessed as previously described (24). Tissue sections were obtained at regular intervals throughout the length of the muscles and ground into powder. The tissue powder was lysed with 200 μ l of RIPA buffer. Immunoblot analysis was performed using 250 μ g of total protein. Protein isolated from age-matching C57BL/10J TA muscles and mixed with protein isolated from uninjected *mdx* muscles to a final concentration of

250 μg were used as a positive control. The dystrophin protein was detected by western blotting as described above using the DYS2 monoclonal antibody (Vector, Inc., Burlingame, CA, USA; 1:200). α -Actinin was used as a sample loading control and was detected using a mouse monoclonal anti-actinin antibody (Sigma; 1:500).

Immunofluorescence analyses

Samples were de-identified and analyzed anonymously. Dystrophin immunostaining of cultured cells was performed as previously described (25). Briefly, cells cultured on cover slips were fixed in ice-cold ethanol for 10 min, rinsed in PBS and permeabilized in 0.3% Triton X-100 for 10 min at room temperature. A solution containing 5% heat-inactivated normal goat serum and 1 mg/ml BSA in PBS was used as blocking solution for 30 min. Cells were incubated with primary antibody to dystrophin (MANDYS-8; 1:200) overnight at 4°C. Cells were washed in PBS before incubation for 1 h at room temperature with an Alexa 546-coupled goat-anti-mouse (H+L) (Molecular Probes; 1:250) secondary antibody. Cover slips were mounted using Vecta Shield (Vector, Inc.) for fluorescence microscopy.

Dystrophin and β -dystroglycan staining of muscles were done using serial 10 μm sections. All muscles were cut for at least two-thirds of the muscle length at intervals of 400 μm and examined for expressions. Sections from different treatment groups were immunoassayed in parallel. Air-dried sections were rehydrated in physiologic solutions and blocked with a solution containing normal goat serum for dystrophin and bovine serum albumin for β -dystroglycan staining diluted 1:20 in PBS. Consecutive sections isolated from muscles were immunoassayed using a rabbit polyclonal antibody (1:200) against dystrophin protein (a generous gift of Dr Qi-Long Lu, University of North Carolina, Chapel Hill, NC, USA) and an antibody against β -dystroglycan (C-20, Santa Cruz; 1:50). Specific antibody bindings were detected with the Alexa 546-coupled goat-anti-rabbit (1:500) and Alexa 488-coupled donkey-anti-goat (1:250) secondary antibodies, respectively.

Digital images were acquired using a CDD Spot RT3 digital camera and Spot Advanced Plus Software Version 4.7 (both from SPOT™ Imaging Solutions, Sterling Heights, MI, USA) interfaced with a Zeiss AxioSkop fluorescence microscope. Images from parallel sections were acquired using the same illumination and image acquisition settings to allow comparison between individual treatment groups. Dystrophin-positive fibers were determined for each muscle cross-section and the number of positives in the section containing the highest number was averaged for each muscle group (Figs 3B and 5A).

Quantitative measurements of muscle fibers

The number of central nuclei were determined in sections immunostained for dystrophin and counterstained with 4'-6-Diamidino-2-phenylindole, dihydrochloride (DAPI, Invitrogen). For each muscle, 200 fibers per section were analyzed. Statistical analysis was performed by comparing the percentage of fibers containing central nuclei from each muscle analyzed within the experimental groups.

Myofiber cross-sectional area was obtained by measuring 150–200 randomly selected fibers per sample. Quantitative analysis was performed using the Image J 1.37c software (National Institute of Health, USA). Analyses were performed by investigators blinded to the treatment.

Forelimb grip strength and wire tests

Treatment groups were assigned a unique identification number and experiments were performed on de-identified mice. Forelimb grip strength was measured using grip strength meter Chatillon DFIS2 (AMETEK, Sellersville, PA, USA). In each trial, the mouse was allowed to grasp a metal rod and the experimenter slowly pulled the mouse by the tail until the digital gauge recorded the peak tension (in Newtons) produced. Five trials were performed with a minimum of 30 s rest in between. Upon completion of the grip strength test, the body weight was recorded. For analysis, peak tension produced in all five trials was averaged and normalized to body weight (47).

Mice were tested for grip strength using a wire apparatus suspended 2 feet from the base. The wire test was made up of five trials, with each trial consisting of a hanging period of 60 s followed by a rest period of 1 min. Animals held on to the wire using all four limbs although, as they weakened, they tended to hold on with only two limbs prior to falling off the wire. The hanging time was recorded for each trial and the best three times (expressed in seconds) were averaged (47).

Toxicity test

Mice that received RTC13 systemically were examined for the presence of toxic effects after single dose or after prolonged administration of compound intraperitoneally. Blood was collected post-mortem and was drawn from the chest cavity after excising the heart. After incubation at room temperature for 30 min to allow for clotting, blood was microcentrifuged at 3000 rpm for 10 min, and the supernatant (serum) was removed and stored at -70°C until use. Age-matched untreated controls and DMSO-treated animals were used for comparison. Biochemical tests for liver and kidney functions were carried out using a VetACE Clinical Chemistry System (Alfa Wasserman Diagnostic Technology LLC, West Caldwell, NJ, USA) and VetAce reagents according to the manufacturer's instructions. Histopathological changes in the liver were assessed using previously published scoring criteria (48). Changes in kidneys were assessed using a scoring criteria ranging from 0 to 3 as follows: 0, no histopathological change; 1 (minimal), glomerular mesangial proliferation and congestion; 2 (moderate), thickening of the basal membrane, intratubular mass and interstitial cell infiltration; 3 (severe), thickening of basal membrane and widespread tubular nephrosis (49). Clinical observations, body weights, food consumptions, organ weights, gross necropsy observations, histopathologic findings and dose administration documentation were recorded and processed according to the Clinical Pathology Laboratories procedures.

Biodistribution studies

Experiments were conducted in *mdx* mice at 6 weeks of age. Animals received a single dose of RTC13 or PTC124 at a concentration of 30 mg/kg and blood and tissues were isolated 30 min, 60 min, 4 h, 24 h, and 5 days after injection. Blood samples were placed into tubes containing lithium–heparin as an anticoagulant, and centrifuged immediately. All muscles and internal tissues were harvested following blood collections. Internal tissues were washed three times with 0.9% NaCl, wiped with filter paper, weighed and flash frozen in liquid nitrogen. Tissues were stored in -80°C until analysis. Samples were prepared by liquid–liquid extraction using validated methods (50,51). Quality control samples were included in each preparation to assess intra-day and inter-day precision and accuracy, as well as recovery and stability. Each analytical batch contained one set of calibration standards, three quality control samples, a blank for each of the RTCs to be analyzed and the study samples. Extraction of RTCs from blood was performed by mixing 50 μl of plasma with 10 μl of 1 M HCl and 1 ml of ethyl-acetate. Samples were vortexed and centrifuged at 5500 rpm for 10 min. Extraction of compounds from tissues was performed as previously described (51). Briefly, tissues were homogenized in 200 μl of a solution containing 0.9% NaCl and proteins were precipitated using 600 μl of ice-cold acetonitrile. Samples were vortexed for 2 min and then centrifuged at 14 000 rpm for 10 min. Organic phases collected from both extraction methods were dried and the residue from each sample was reconstituted with 100 μl of DMSO, vortexed for 5 min and centrifuged at 14 000 rpm for 10 min. Finally, 10 μl of the supernatant was injected for liquid chromatography mass spectrometry (LCMS) analysis.

LCMS experiments were carried out on a Waters Acquity UPLC connected to a Waters LCT-Premier XE Time of Flight mass spectrometer controlled by the MassLynx 4.1 software (all from Waters Corporation, Milford, MA, USA). The mass spectrometer was equipped with a Multi-Mode Source operated in the electrospray mode. Acquity BEH C18 2.1 \times 50 mM, UPLC column (Waters Corporation). The mobile phase was as follows: 2% B for 1.5 min, a ramp of 2–95% B from 1.5 to 5 min and 95% B from 5 to 6.5 min (solvent A: water, solvent B: acetonitrile). Mass spectra were recorded from m/z 70 to 1500. The instrument response for PTC124 was measured by generating extracted ion chromatograms for ions at $-m/z$ 283 and 589 with a mass window of 1 Da, integrating the trace at RT 4.6 min and adding the integrated values. An analogous process was used for RTC13 with m/z 316 and 631 and RT = 4.9 min.

Calibration standards were prepared in ranges of 1 to 100 $\mu\text{g}/\text{ml}$ for plasma and 1 to 100 $\mu\text{g}/\text{g}$ for tissues and were generated by adding the working solution to the samples to be analyzed followed by immediate extraction. The linearity of the relationship between the detector response and the concentrations of PTC124 and RTC13 was confirmed within the concentration range of 5 and 100 $\mu\text{g}/\text{ml}$ for mouse blood and 10 to 100 $\mu\text{g}/\text{mg}$ for the liver, kidney, heart and skeletal muscles homogenates. Calibration curves were calculated by performing a linear regression (weighted $1/x^2$) on the calibration standards. The precision of the method was estimated by calculating the values for mean, standard deviation

(SD) and the coefficient of variation (%CV) which was obtained by dividing the SD by the mean of each batch and multiplying the value by 100. The accuracy of the assay was assessed by comparing the calculated mean concentrations to the actual concentrations of serial dilutions and was expressed as percentage of relative error (%RE). The %CV for the QC samples in the assay of RTC13 ranged from 2.70 to 5.03% and the %RE ranged from -6.76 to 4.39%. The precision of calibration standards for RTC13 ranged from 3.70 to 6.2% and %RE ranged from -9.28 to 4.05%. In the assay for PTC124, the precision ranged from 2.13 to 7.45% and the accuracy ranged between -2.70 and 5.49%. The precision of sample replicates for RTC13 ranged from 4.4 to 9.4% and for PTC124 2.9 to 6.3%. The correlation coefficient of the calibration standards was >0.999 for both RTC13 and PTC124.

CK assays

Blood was isolated as described above. CK serum activities were determined using a Biotron kit following the manufacturer's instructions. All assays were performed in duplicate and all sera were diluted 1:20 prior to assay. Blood that was hemolyzed (as judged by a blinded observer) was excluded from the analysis. Values are reported as international units.

Statistical analysis

Data are presented as means and standard deviations. Comparisons between groups were done using Student's *t*-test assuming two-tailed distribution and unequal variances.

SUPPLEMENTARY MATERIAL

Supplementary Material is available at *HMG* online.

ACKNOWLEDGEMENTS

The authors would like to thank Dr Richard Gatti for providing the RTC14 and RTC13 (funded by a National Institutes of Health grant 1R01NS052528) that were used for the *in vitro* experiments in *mdx* myotubes and for helpful suggestions and critical discussion of the manuscript, Dr Melissa Spencer and the Mouse Muscle Phenotyping and Imaging Core for assistance with grip strength and wire testing of mice (funded by NIAMS P30AR057230-01), Dr Joseph Loo at the Department of Chemistry and Biochemistry for assistance with the biodistribution studies (supported by a grant from the National Center for Research Resources S10RR025631) and Dr Nora Rozengurt, at the CURE DDRC Morphology and Imaging CORE Service for the histological analysis of the mice tissues. The authors have no conflicting financial interests.

Conflict of Interest statement. None declared.

FUNDING

The work was supported by a grant from the Muscular Dystrophy Association (184494) to C.B.

AUTHOR CONTRIBUTION

R.K. performed experiments *in vivo*, analyzed data and wrote the manuscript. C.B. designed and directed the study, performed the experiments *in vitro* analyzed and integrated the data and wrote the manuscript. O.P. contributed the data on toxicology and muscle physiology studies. G.K. developed the LC-MS method and assisted with the biodistribution studies. J.-M.K. and M.J. produced PTC124, RTC14 and part of the RTC13 compounds used in the study.

REFERENCES

- Monaco, A.P., Neve, R.L., Colletti-Feener, C., Bertelson, C.J., Kurnit, D.M. and Kunkel, L.M. (1986) Isolation of candidate cDNAs for portions of the Duchenne muscular dystrophy gene. *Nature*, **323**, 646–650.
- Prior, T.W., Bartolo, C., Pearl, D.K., Papp, A.C., Snyder, P.J., Sedra, M.S., Burghes, A.H. and Mendell, J.R. (1995) Spectrum of small mutations in the dystrophin coding region. *Am. J. Hum. Genet.*, **57**, 22–33.
- Mendell, J.R., Buzin, C.H., Feng, J., Yan, J., Serrano, C., Sangani, D.S., Wall, C., Prior, T.W. and Sommer, S.S. (2001) Diagnosis of Duchenne dystrophy by enhanced detection of small mutations. *Neurology*, **57**, 645–650.
- Sicinski, P., Geng, Y., Ryder-Cook, A.S., Barnard, E.A., Darlison, M.G. and Barnard, P.J. (1989) The molecular basis of muscular dystrophy in the mdx mouse: a point mutation. *Science*, **244**, 1578–1580.
- Phelps, S.F., Hauser, M.A., Cole, N.M., Rafael, J.A., Hinkle, R.T., Faulkner, J.A. and Chamberlain, J.S. (1995) Expression of full-length and truncated dystrophin mini-genes in transgenic mdx mice. *Hum. Mol. Genet.*, **4**, 1251–1258.
- Barton-Davis, E.R., Cordier, L., Shoturma, D.I., Leland, S.E. and Sweeney, H.L. (1999) Aminoglycoside antibiotics restore dystrophin function to skeletal muscles of mdx mice. *J. Clin. Invest.*, **104**, 375–381.
- Wagner, K.R., Hamed, S., Hadley, D.W., Gropman, A.L., Burstein, A.H., Escolar, D.M., Hoffman, E.P. and Fischbeck, K.H. (2001) Gentamicin treatment of Duchenne and Becker muscular dystrophy due to nonsense mutations. *Ann. Neurol.*, **49**, 706–711.
- Keeling, K.M., Brooks, D.A., Hopwood, J.J., Li, P., Thompson, J.N. and Bedwell, D.M. (2001) Gentamicin-mediated suppression of Hurler syndrome stop mutations restores a low level of alpha-L-iduronidase activity and reduces lysosomal glycosaminoglycan accumulation. *Hum. Mol. Genet.*, **10**, 291–299.
- Du, M., Jones, J.R., Lanier, J., Keeling, K.M., Lindsey, J.R., Tousson, A., Bebek, Z., Whitsett, J.A., Dey, C.R., Colledge, W.H. *et al.* (2002) Aminoglycoside suppression of a premature stop mutation in a Cfr^{-/-} mouse carrying a human CFTR-G542X transgene. *J. Mol. Med.*, **80**, 595–604.
- Politano, L., Nigro, G., Nigro, V., Piluso, G., Papparella, S., Paciello, O. and Comi, L.I. (2003) Gentamicin administration in Duchenne patients with premature stop codon. Preliminary results. *Acta Myol.*, **22**, 15–21.
- Lai, C.H., Chun, H.H., Nahas, S.A., Mitui, M., Gamo, K.M., Du, L. and Gatti, R.A. (2004) Correction of ATM gene function by aminoglycoside-induced read-through of premature termination codons. *Proc. Natl Acad. Sci. USA.*, **101**, 15676–15681.
- Weiner, A.M. and Weber, K. (1973) A single UGA codon functions as a natural termination signal in the coliphage q beta coat protein cistron. *J. Mol. Biol.*, **80**, 837–855.
- Lovett, P.S. (1991) Ribosomal RNA and the site specificity of chloramphenicol-dependent ribosome stalling in cat gene leaders. *Ann. N. Y. Acad. Sci.*, **646**, 31–34.
- Manuvakhova, M., Keeling, K. and Bedwell, D.M. (2000) Aminoglycoside antibiotics mediate context-dependent suppression of termination codons in a mammalian translation system. *RNA*, **6**, 1044–1055.
- Malik, V., Rodino-Klapac, L.R., Viollet, L. and Mendell, J.R. (2010) Aminoglycoside-induced mutation suppression (stop codon readthrough) as a therapeutic strategy for Duchenne muscular dystrophy. *Ther. Adv. Neurol. Disord.*, **3**, 379–389.
- Wilschanski, M., Yahav, Y., Yaacov, Y., Blau, H., Bentur, L., Rivlin, J., Aviram, M., Bdolah-Abram, T., Bebok, Z., Shushi, L. *et al.* (2003) Gentamicin-induced correction of CFTR function in patients with cystic fibrosis and CFTR stop mutations. *N. Engl. J. Med.*, **349**, 1433–1441.
- Welch, E.M., Barton, E.R., Zhuo, J., Tomizawa, Y., Friesen, W.J., Trifillis, P., Paushkin, S., Patel, M., Trotta, C.R., Hwang, S. *et al.* (2007) PTC124 targets genetic disorders caused by nonsense mutations. *Nature*, **447**, 87–91.
- Auld, D.S., Thorne, N., Maguire, W.F. and Inglese, J. (2009) Mechanism of PTC124 activity in cell-based luciferase assays of nonsense codon suppression. *Proc. Natl Acad. Sci. USA.*, **106**, 3585–3590.
- Peltz, S.W., Welch, E.M., Jacobson, A., Trotta, C.R., Naryshkin, N., Sweeney, H.L. and Bedwell, D.M. (2009) Nonsense suppression activity of PTC124 (ataluren). *Proc. Natl Acad. Sci. USA*, **106**, E64.
- Auld, D.S., Lovell, S., Thorne, N., Lea, W.A., Maloney, D.J., Shen, M., Rai, G., Battaile, K.P., Thomas, C.J., Simeonov, A. *et al.* (2010) Molecular basis for the high-affinity binding and stabilization of firefly luciferase by PTC124. *Proc. Natl Acad. Sci. USA*, **107**, 4878–4883.
- Thorne, N., Inglese, J. and Auld, D.S. (2010) Illuminating insights into firefly luciferase and other bioluminescent reporters used in chemical biology. *Chem. Biol.*, **17**, 646–657.
- Sermet-Gaudelus, I., De, B.K., Casimir, G.J., Vermeulen, F., Leal, T., Mogenet, A., Roussel, D., Fritsch, J., Hanssens, L., Hirawat, S. *et al.* (2010) Ataluren (PTC124) induces CFTR protein expression and activity in children with nonsense mutation cystic fibrosis. *Am. J. Respir. Crit. Care Med.*, **182**, 1262–1272.
- Du, L., Damoiseaux, R., Nahas, S., Gao, K., Hu, H., Pollard, J.M., Goldstine, J., Jung, M.E., Henning, S.M., Bertoni, C. and Gatti, R.A. (2009) Nonaminoglycoside compounds induce readthrough of nonsense mutations. *J. Exp. Med.*, **206**, 2285–2297.
- Kayali, R., Bury, F., Ballard, M. and Bertoni, C. (2010) Site directed gene repair of the dystrophin gene mediated by PNA-ssODNs. *Hum. Mol. Genet.*, **19**, 3266–3281.
- Bertoni, C., Morris, G.E. and Rando, T.A. (2005) Strand bias in oligonucleotide-mediated dystrophin gene editing. *Hum. Mol. Genet.*, **14**, 221–233.
- Bertoni, C. and Rando, T.A. (2002) Dystrophin gene repair in mdx muscle precursor cells in vitro and in vivo mediated by RNA-DNA chimeric oligonucleotides. *Hum. Gene Ther.*, **13**, 707–718.
- Ohlndieck, K. and Campbell, K.P. (1991) Dystrophin-associated proteins are greatly reduced in skeletal muscle from mdx mice. *J. Cell Biol.*, **115**, 1685–1694.
- Meyer, O.A., Tilson, H.A., Byrd, W.C. and Riley, M.T. (1979) A method for the routine assessment of fore- and hindlimb grip strength of rats and mice. *Neurobehav. Toxicol.*, **1**, 233–236.
- Connolly, A.M., Keeling, R.M., Mehta, S., Pestronk, A. and Sanes, J.R. (2001) Three mouse models of muscular dystrophy: the natural history of strength and fatigue in dystrophin-, dystrophin/utrophin-, and laminin [alpha]2-deficient mice. *Neuromuscul. Disord.*, **11**, 703–712.
- Gomez, C.M., Maselli, R., Gundeck, J.E., Chao, M., Day, J.W., Tamamizu, S., Lasalde, J.A., McNamee, M. and Wollmann, R.L. (1997) Slow-channel transgenic mice: a model of postsynaptic organellar degeneration at the neuromuscular junction. *J. Neurosci.*, **17**, 4170–4179.
- Rafael, J.A., Nitta, Y., Peters, J. and Davies, K.E. (2000) Testing of SHIRPA, a mouse phenotypic assessment protocol, on Dmd(mdx) and Dmd(mdx3cv) dystrophin-deficient mice. *Mamm. Genome*, **11**, 725–728.
- van Putten, M., de Winter, C., van Roon-Mom, W., van Ommen, G.J., 'T Hoen, P.A. and Aartsma-Rus, A. (2010) A 3 months mild functional test regime does not affect disease parameters in young mdx mice. *Neuromuscul. Disord.*, **20**, 273–280.
- Schnell, M.A., Hardy, C., Hawley, M., Propert, K.J. and Wilson, J.M. (2002) Effect of blood collection technique in mice on clinical pathology parameters. *Hum. Gene Ther.*, **13**, 155–161.
- Spurney, C.F., Gordish-Dressman, H., Guerron, A.D., Sali, A., Pandey, G.S., Rawat, R., Van Der Meulen, J.H., Cha, H.J., Pistilli, E.E., Partridge, T.A. *et al.* (2009) Preclinical drug trials in the mdx mouse: assessment of reliable and sensitive outcome measures. *Muscle Nerve*, **39**, 591–602.

35. Rooney, J.E., Gurpur, P.B. and Burkin, D.J. (2009) Laminin-111 protein therapy prevents muscle disease in the mdx mouse model for Duchenne muscular dystrophy. *Proc. Natl Acad. Sci. USA*, **106**, 7991–7996.
36. Brazeau, G.A., Mathew, M. and Entrikin, R.K. (1992) Serum and organ indices of the mdx dystrophic mouse. *Res. Commun. Chem. Pathol. Pharmacol.*, **77**, 179–189.
37. Jung, M.E., Ku, J.M., Du, L., Hu, H. and Gatti, R.A. (2011) Synthesis and evaluation of compounds that induce readthrough of premature termination codons. *Bioorg. Med. Chem. Lett.*, **21**, 5842–5848.
38. Hirawat, S., Welch, E.M., Elfring, G.L., Northcutt, V.J., Paushkin, S., Hwang, S., Leonard, E.M., Almstead, N.G., Ju, W., Peltz, S.W. *et al.* (2007) Safety, tolerability, and pharmacokinetics of PTC124, a nonaminoglycoside nonsense mutation suppressor, following single- and multiple-dose administration to healthy male and female adult volunteers. *J. Clin. Pharmacol.*, **47**, 430–444.
39. Akimitsu, N. (2008) Messenger RNA surveillance systems monitoring proper translation termination. *J. Biochem.*, **143**, 1–8.
40. Chang, Y.F., Imam, J.S. and Wilkinson, M.F. (2007) The nonsense-mediated decay RNA surveillance pathway. *Annu. Rev. Biochem.*, **76**, 51–74.
41. Amrani, N., Sachs, M.S. and Jacobson, A. (2006) Early nonsense: mRNA decay solves a translational problem. *Nat. Rev. Mol. Cell Biol.*, **7**, 415–425.
42. Ahmad, A., Brinson, M., Hodges, B.L., Chamberlain, J.S. and Amalfitano, A. (2000) Mdx mice inducibly expressing dystrophin provide insights into the potential of gene therapy for duchenne muscular dystrophy. *Hum. Mol. Genet.*, **9**, 2507–2515.
43. Alter, J., Lou, F., Rabinowitz, A., Yin, H., Rosenfeld, J., Wilton, S.D., Partridge, T.A. and Lu, Q.L. (2006) Systemic delivery of morpholino oligonucleotide restores dystrophin expression bodywide and improves dystrophic pathology. *Nat. Med.*, **12**, 175–177.
44. Bertoni, C., Jarrahan, S., Wheeler, T.M., Li, Y., Olivares, E.C., Calos, M.P. and Rando, T.A. (2006) Enhancement of plasmid-mediated gene therapy for muscular dystrophy by directed plasmid integration. *Proc. Natl Acad. Sci. USA*, **103**, 419–424.
45. Yin, H., Lu, Q. and Wood, M. (2008) Effective exon skipping and restoration of dystrophin expression by peptide nucleic acid antisense oligonucleotides in mdx mice. *Mol. Ther.*, **16**, 38–45.
46. Bertoni, C., Lau, C. and Rando, T.A. (2003) Restoration of dystrophin expression in mdx muscle cells by chimeraplast-mediated exon skipping. *Hum. Mol. Genet.*, **12**, 1087–1099.
47. Vetrone, S.A., Montecino-Rodriguez, E., Kudryashova, E., Kramerova, I., Hoffman, E.P., Liu, S.D., Miceli, M.C. and Spencer, M.J. (2009) Osteopontin promotes fibrosis in dystrophic mouse muscle by modulating immune cell subsets and intramuscular TGF-beta. *J. Clin. Invest.*, **119**, 1583–1594.
48. Tsimoyiannis, E.C., Moutesidou, K.J., Moschos, C.M., Karayianni, M., Karkabounas, S. and Kotoulas, O.B. (1993) Trimetazidine for prevention of hepatic injury induced by ischaemia and reperfusion in rats. *Eur. J. Surg.*, **159**, 89–93.
49. Shigematsu, H. (1997) Histological grading and staging of IgA nephropathy. *Pathol. Int.*, **47**, 194–202.
50. Watanabe, E., Mochizuki, N., Ajima, H., Ohno, K., Shiino, M., Umezawa, K., Fukai, M., Ozaki, M., Furukawa, H., Todo, S. *et al.* (2008) A simple and reliable method for determining plasma concentration of dehydroxymethylepoxyquinomicin by high performance liquid chromatography with mass spectrometry. *J. Chromatogr. B Analyt. Technol. Biomed. Life Sci.*, **871**, 32–36.
51. Li, H., Ezell, S.J., Zhang, X., Wang, W., Xu, H., Rayburn, E.R., Zhang, X., Gurpinar, E., Yang, X., Sommers, C.I. *et al.* (2011) Development and validation of an HPLC method for quantitation of BA-TPQ, a novel iminoquinone anticancer agent, and an initial pharmacokinetic study in mice. *Biomed. Chromatogr.*, **25**, 628–634.